Breakup of Temperature Inversions in Deep Mountain Valleys: Part II. Thermodynamic Model

C. DAVID WHITEMAN

Pacific Northwest Laboratory, Richland, WA 99352

THOMAS B. MCKEE

Department of Atmospheric Science, Colorado State University, Fort Collins 80523

(Manuscript received 31 March 1981, in final form 7 December 1981)

ABSTRACT

A thermodynamic model is developed to simulate the evolution of vertical temperature structure during the breakup of nocturnal temperature inversions in mountain valleys. The primary inputs to the model are the valley floor width, sidewall inclination angles, characteristics of the valley inversion at sunrise, and an estimate of sensible heat flux obtained from solar radiation calculations. The outputs, obtained by a numerical integration of the model equations, are the time-dependent height of a convective boundary layer that grows upward from the valley floor after sunrise, the height of the inversion top, and vertical potential temperature profiles of the valley atmosphere. The model can simulate the three patterns of temperature structure evolution observed in deep valleys of western Colorado. The well-known inversion breakup over flat terrain is a special case of the model, for which valley floor width becomes infinite. The characteristics of the model equations are investigated for several limiting conditions using the topography of a reference valley and typical inversion and solar radiation characteristics. The model is applied to simulate observations of inversion breakup taken in Colorado's Eagle and Yampa Valleys in different seasons. Simulations are obtained by fitting two constants in the model, relating to the surface energy budget and energy partitioning, to the data. The model accurately simulates the evolution of vertical potential temperature profiles and predicts the time of inversion destruction.

1. Introduction

In Part I (Whiteman, 1982) observations of vertical temperature structure and wind evolution were summarized for 21 case studies of nocturnal temperature inversion breakup in deep Colorado mountain valleys. Breakup occurred following one of three patterns of vertical temperature structure evolution. A hypothesis was offered to explain the observations in which sensible heat flux was the driving force and one of the three patterns occurred, depending on whether the sensible heat flux was used primarily to cause convective boundary layers (CBLs) to grow over the valley floor and sidewalls (Pattern 1), to remove mass from the inversion in the upslope flows (Pattern 2), or to accomplish both (Pattern 3). In Part II, a bulk thermodynamic model of temperature inversion destruction is developed based on the hypothesis, using several simplifying assumptions.

2. Mathematical model of inversion destruction

a. General equations

Two approaches can be used to develop a mathematical model able to simulate temperature changes in the valley atmosphere. In the first approach detailed mathematical equations can be developed for the individual components of the overall system, including the various boundary layers and stable core. However, the valley atmosphere consists of many interrelated layers, and the coupling of the equations for the different layers to simulate potential temperature changes in the valley atmosphere as a whole would be difficult due to geometrical considerations and lack of detailed information on physical characteristics of the various layers. Consequently, a second approach is taken in which a bulk thermodynamic model is developed for the valley inversion. As more is learned about the individual components of the system, the model can be refined to introduce greater detail into the simulation of the individual components.

The thermodynamic model of valley temperature structure evolution developed here is based on the hypothesis of Part I. Fig. 1 shows a unit thick cross section of a mountain valley having sidewalls of inclination α_1 and α_2 and valley floor width l. At sunrise (t_i) the valley is assumed to have an inversion of depth h_i and constant vertical potential temperature gradient γ. The variable width of the valley at the

0021-8952/82/030290-13$07.25

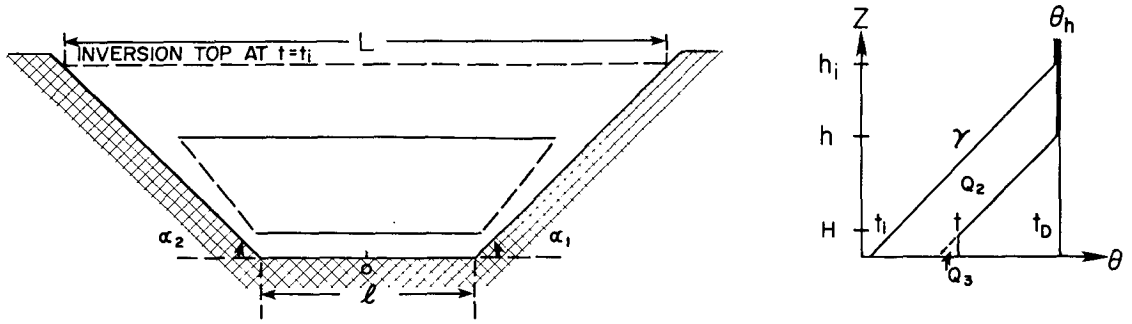

FIG. 1. Valley geometry and potential temperature profiles used to formulate a mathematical model of inversion destruction.

top of the inversion is designated by L, and the origin of a y-z coordinate system is placed at the center of the valley floor at point 0. After sunrise a typical Pattern 3 potential temperature evolution ensues, in which a CBL develops over the valley floor and sidewalls. Removal of mass from the valley in these CBLs allows the stable core to sink so that a sounding taken at an arbitrary later time t will show a lower inversion top height $h(t)$ and a shallow CBL of height $H(t)$ near the ground. A later sounding, taken at a time t_D when the inversion has just been destroyed, will show a neutral atmosphere having a potential temperature $\theta = \theta_h$.

From the first law of thermodynamics, the increment of energy required to increase the potential temperature of a mass of air m by the potential temperature increment $\Delta\theta$ is

$$\Delta Q = mc_p \frac{T}{\theta}\Delta\theta = \rho V c_p \frac{T}{\theta}\Delta\theta, \tag{1}$$

where $T/\theta = (P/1000)^{R/c_p} \approx 1$, ρ is the density (assumed constant) and V is volume. Using (1), the energy required to change the valley potential temperature profile at time t_i to the profile at time t can be obtained by an integration over the valley volume below the height of the inversion top. The total energy requirement is composed of two parts: the energy increment Q_2 that removes mass from the valley and allows the top of the inversion to sink, and the energy increment Q_3 that causes a CBL to grow. These energies are represented by the areas designated in Fig. 1 and are given by

$$Q_2 = \rho c_p \frac{T}{\theta}\left[\int_0^{h_i}\int_{y_L}^{y_R}\int_0^1 \Delta\theta_i dx dy dz - \int_0^{h}\int_{y_L}^{y_R}\int_0^1 \Delta\theta_1 dx dy dz\right], \tag{2}$$

$$= \rho c_p \frac{T}{\theta}\gamma\left[\frac{l}{2}(h_i^2 - h^2) + \frac{C}{6}(h_i^3 - h^3)\right], \tag{3}$$

where

$$\Delta\theta_i = \gamma(h_i - z), \tag{4}$$

$$y_L = -\left(\frac{l}{2} + \frac{z}{\tan\alpha_2}\right), \tag{5}$$

$$y_R = \frac{l}{2} + \frac{z}{\tan\alpha_1}, \tag{6}$$

$$C = \frac{1}{\tan\alpha_1} + \frac{1}{\tan\alpha_2}, \tag{7}$$

$$\Delta\theta_1 = \gamma(h - z), \tag{8}$$

and

$$Q_3 = \rho c_p \frac{T}{\theta}\int_0^H\int_{y_L}^{y_R}\int_0^1 \Delta\theta_2 dx dy dz, \tag{9}$$

$$= \rho c_p \frac{T}{\theta}\gamma\left[\frac{l}{2}H^2 + \frac{C}{6}H^3\right], \tag{10}$$

where

$$\Delta\theta_2 = \gamma(H - z). \tag{11}$$

In order to simplify the integration, it was assumed that the valley temperature structure is horizontally homogeneous across the valley, that mass is removed from the valley in such a way that the potential temperature gradient in the inversion layer does not change with time, and that ρ and c_p are constant. By differentiating the individual energies Q_2 and Q_3 with respect to time, the rates of change of the height of the top of the inversion and the height of the CBL are obtained, such that

$$\frac{dQ_2}{dt} = \rho c_p \frac{T}{\theta}\gamma\left[-h\frac{dh}{dt}\left(l + \frac{hC}{2}\right)\right], \tag{12}$$

$$\frac{dQ_3}{dt} = \rho c_p \frac{T}{\theta}\gamma\left[H\frac{dH}{dt}\left(l + \frac{HC}{2}\right)\right]. \tag{13}$$

The total rate of energy input into the valley to accomplish these changes is the fraction A_0 of solar irradiance F coming across the area L of the top of the inversion that is converted to sensible heat. The solar irradiance may be approximated by a sine function having a certain amplitude A_1 and period τ, so that the total rate of energy input becomes

$$\frac{dQ_1}{dt} = A_0 LF = A_0(l + hC)A_1 \sin\frac{\pi}{\tau}(t - t_i). \tag{14}$$

An energy balance for the valley inversion is obtained by equating (14) to the sum of (12) and (13). Alternatively, a fraction of the energy input is available to drive the growth of the CBL while the rest of the incoming energy is used to remove mass from the valley. The fraction of energy input used to drive the CBL growth is assumed to be of the form

$$k\left(\frac{l+HC}{l+hC}\right),$$

where k is a number between 0 and 1. This form is chosen in order to simplify later equations. Equating this fraction of the energy input to (12) and the remainder to (13) and solving for dH/dt and dh/dt results in the final model equations

$$\frac{dH}{dt} = \frac{\theta}{T}\frac{k}{\rho c_p}\left(\frac{l+HC}{l+\tfrac{1}{2}HC}\right) \times \frac{A_0A_1}{\gamma H}\sin\left[\frac{\pi}{\tau}(t-t_i)\right], \quad (15)$$

$$\frac{dh}{dt} = -\frac{\theta}{T}\frac{1}{\rho c_p}\left[\frac{l+hC-k(l+HC)}{l+\tfrac{1}{2}hC}\right] \times \frac{A_0A_1}{\gamma h}\sin\left[\frac{\pi}{\tau}(t-t_i)\right]. \quad (16)$$

These equations specify the dependence of the rate of ascent of the CBL and the rate of descent of the inversion top on inversion characteristics, incoming energy and valley topography. An integration of the coupled equations allows the simulation of the time-dependent behavior of the heights of the CBL and inversion top. If the potential temperature θ_h at the top of the inversion is known and is independent of time, and γ is constant, knowledge of the variation of h and H with time is sufficient to specify how vertical profiles of potential temperature change with time. When $k = 0$, the equations provide an approximate simulation of Pattern 2 inversion destruction in which destruction occurs solely due to the removal of mass from a valley in the slope flows, resulting in a descent of the inversion top. When $k = 1$, the equations provide a simulation of Pattern 1 inversion destruction, in which destruction occurs mainly due to the growth of a CBL over the valley floor. When $k = 1$ and the valley floor becomes very wide, the simulation approaches that of inversion destruction over the plains. When k is between 0 and 1, the equations provide a simulation of Pattern 3 inversion destruction in which the inversion is destroyed by the combined effect of a growing CBL and a descending inversion top. A more complete description of the characteristics of the model equations for Pattern 1, 2 and 3 temperature structure evolution follows.

b. Pattern 2 inversion destruction

The physical hypothesis of Pattern 2 inversion destruction requires a shallow CBL to form over the sidewalls so that additional energy can be used to cause mass to flow up them. Pattern 2 destruction may be approximated by assuming that all the energy available to destroy the inversion goes solely to move mass up the sidewalls, causing the top of the inversion to descend. This can be accomplished by setting k equal to zero in (15) and (16) resulting in the two equations

$$\frac{dH}{dt} = 0, \quad (17)$$

$$\frac{dh}{dt} = -\frac{\theta}{T}\left(\frac{l+hC}{l+\tfrac{1}{2}hC}\right)\frac{A_0A_1}{\rho c_p\gamma h}\sin\left[\frac{\pi}{\tau}(t-t_i)\right]. \quad (18)$$

Following these equations, the CBL does not grow as a function of time, and the inversion is destroyed as the top of the inversion sinks. The rate of descent of the top of the inversion increases as the inversion descends. The descent rate is faster when more energy is available and when the potential temperature gradient of the inversion is weaker. The factor in large parentheses in (18) is a topographic factor that varies from 1 to 2 depending on the shape of the valley cross section. This accounts for the reduced volume of air within the mountain valley relative to that over the plains for the same energy flux on a horizontal surface. Since the valley has less volume to be heated by the same incoming energy, it warms more rapidly. By separating variables h and t and integrating from the initial conditions $h = h_i$ and $H = 0$ at $t = t_i$ to $h = h$ and $H = H$ at $t = t$, analytical expressions are obtained which describe how H and h vary with time, i.e.,

$$H = 0, \quad (19)$$

$$\tfrac{1}{4}(h^2 - h_i^2) + \frac{l}{2C}(h-h_i) + \frac{l^2}{2C^2}\ln\left(\frac{l+h_iC}{l+hC}\right) = \frac{\theta}{T}\frac{A_0A_1}{\rho c_p\gamma}\frac{\tau}{\pi}\left\{\cos\left[\frac{\pi}{\tau}(t-t_i)\right]-1\right\}. \quad (20)$$

Fig. 2 illustrates the shapes of the curves of h vs t for a reference simulation and for two cases where one parameter in the reference simulation is changed. The reference simulation uses representative values of valley parameters observed in western Colorado including $l = 1000$ m, $\alpha_1 = \alpha_2 = 15°$, $h_i = 500$ m, $\gamma = 0.025$ K m^{-1}, $\tau = 12$ h $= 43200$ s, $T/\theta = 1$ and $\rho = 1$ kg m^{-3}. The reference inversion takes nearly 4½ h to be destroyed when $A_0A_1/\rho c_p = 0.25$ K m s^{-1}. Fig. 2 was obtained by a numerical integration of (18) using a forward finite difference scheme and a time step of 10 min.

An analytical expression for the time required to

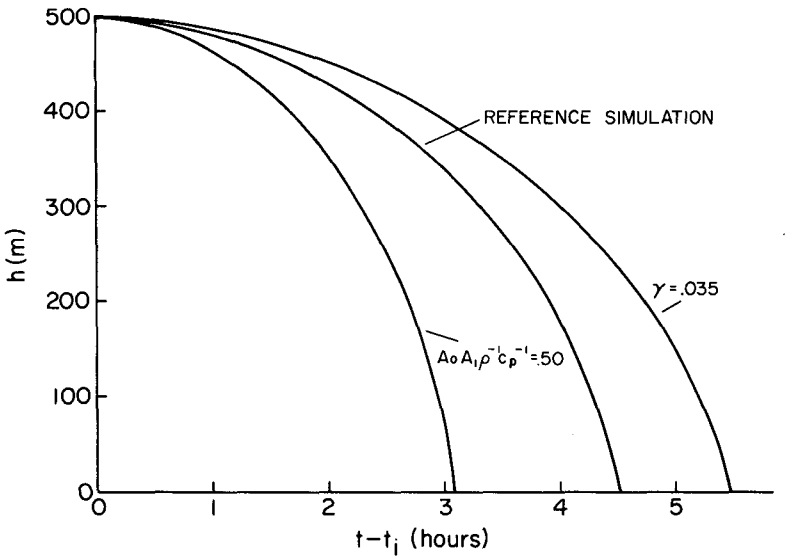

FIG. 2. Descent of inversion top as a function of time for the reference inversion simulation and for two simulations for which the single parameters indicated were changed. Pattern 2 destruction.

destroy an inversion can be obtained by integrating (18) from the initial conditions to the final conditions of $h = 0$ at $t = t_D$. This expression,

$$t_D - t_i = \frac{\tau}{\pi}\cos^{-1}\left\{1 - \frac{T}{\theta}\frac{\rho C_p \gamma}{A_0 A_1}\frac{\pi}{\tau} \times \left[\frac{h_i^2}{4} + \frac{l h_i}{2C} + \frac{l^2}{2C^2}\ln\left(\frac{l}{l + h_i C}\right)\right]\right\}, \quad (21)$$

enumerates the factors affecting inversion breakup time. The sensitivity of inversion breakup time (measured from sunrise) to the various parameters is illustrated in Fig. 3 using the reference simulation above. The reference inversion takes 4.4 h to break (vertical line in Fig. 3). The effect on the time required to destroy the reference inversion by varying the individual parameters is obtained by following the labeled curves. Thus, varying the initial height of the inversion from 400 to 600 m, other parameters being equal, changes the time required to destroy the inversion from 3.5 to 5.4 h. For the reference inversion, the most sensitive parameters affecting the time required to break an inversion are the available energy and the initial potential temperature gradient

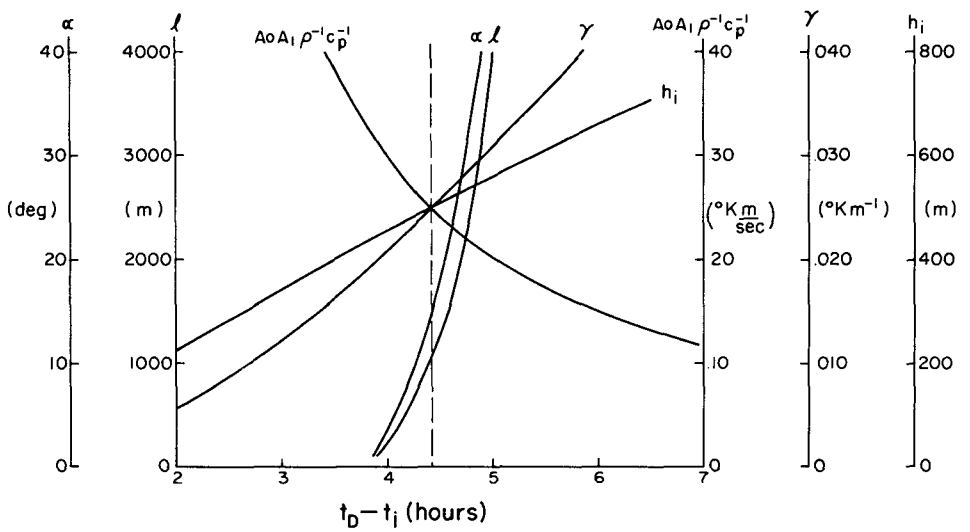

FIG. 3. Sensitivity of inversion destruction time to various model parameters for Pattern 2 destruction.

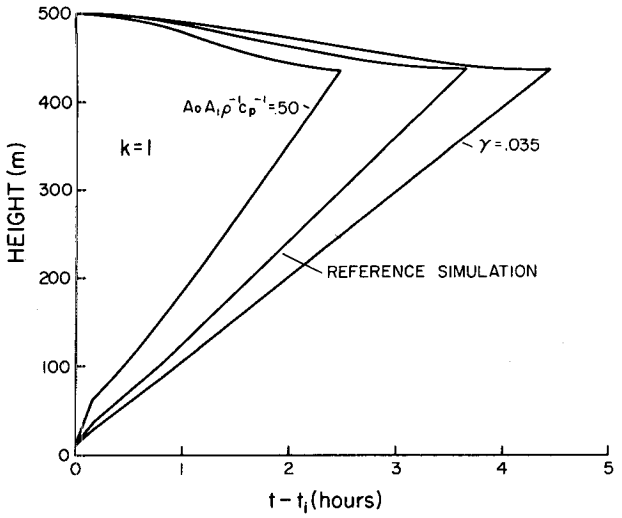

FIG. 4. Ascent of CBL and descent of inversion top as a function of time for Pattern 1 inversion destruction in a valley for the reference simulation and for two simulations in which single parameters were changed to the values indicated.

and inversion height. In the normally dry Colorado valleys the most important factors affecting the available energy are albedo (snow versus no snow) and latent heat flux. The effect of valley shape on the breakup time is relatively small for normal ranges of α and l encountered in valleys of western Colorado. Nevertheless, it is apparent that the valley width and sidewall angles may affect the mode of inversion destruction since they control, to a certain extent, the divergence of mass in the CBL's and thus determine whether inversion destruction more nearly follows Pattern 1 or Pattern 2. Overall, predictions of the time required to destroy inversions, given typical values of the parameters observed in field experiments, are consistent with the observed range of 3.5–5 h.

c. *Pattern 1 inversion destruction—Valley case*

A useful approximation to Pattern 1 inversion destruction can be obtained from the model equations by setting $k = 1$ in (15) and (16). The general equations then reduce to the two equations

$$\frac{dH}{dt} = \frac{\theta}{T}\left(\frac{l + HC}{l + \tfrac{1}{2}HC}\right)\frac{A_0A_1}{\rho c_p\gamma H}\sin\left[\frac{\pi}{\tau}(t - t_i)\right], \quad (22)$$

$$\frac{dh}{dt} = -\frac{\theta}{T}\left[\frac{(h - H)C}{l + \tfrac{1}{2}hC}\right] \times \frac{A_0A_1}{\rho c_p\gamma h}\sin\left[\frac{\pi}{\tau}(t - t_i)\right]. \quad (23)$$

Eq. (22) is formulated so that the entire fraction A_0 of the energy coming across the area $(l + HC)$ of the top of the CBL is used to cause the CBL to grow. The energy used to cause the top of the inversion to descend is the fraction A_0 of the difference between the energy coming across the top of the inversion and the energy coming across the top of the CBL. The time-dependent behavior of the height of the CBL can be obtained by an integration of (22) from the initial condition of $H = 0$ at $t = t_i$ to the final condition of $H = H$ at $t = t$, such that

$$\frac{H^2}{4} + \frac{lH}{2C} + \frac{l^2}{2C^2}\ln\left(\frac{l}{l + HC}\right) = \frac{\theta}{T}\frac{A_0A_1}{\rho c_p\gamma}\frac{\tau}{\pi}\left\{1 - \cos\left[\frac{\pi}{\tau}(t - t_i)\right]\right\}. \quad (24)$$

The integration of (22) and (23) can be accomplished numerically to determine how h and H change with time in a Pattern 1 inversion destruction in a mountain valley. This is done for the reference simulation and for two simulations in which a single parameter of the reference simulation is changed. The resulting plots are shown in Fig. 4. The characteristics of the plots include a near-linear growth of the CBL with time, a slow descent of the inversion top, and a more rapid breakup than for Pattern 2 destruction. Pattern 1 destruction takes 3.7 h versus the 4.4 h required for Pattern 2 breakup. The same total amount of energy is required to destroy the reference inversion, whether it is destroyed following Pattern 1 or Pattern 2. However, since the energy available to destroy the inversion comes across the area of the top of the inversion, and this area is larger when the inversion top sinks more slowly, the total amount of energy required to destroy the inversion is attained earlier in the day, resulting in an earlier inversion breakup.

d. *Pattern 1 inversion destruction—Flat plains case*

Application of (22) and (23) to a valley that is very wide or approaches a plain ($l \to \infty$) results in the equations

$$\frac{dH}{dt} = \frac{\theta}{T}\frac{A_0A_1}{\rho c_p\gamma H}\sin\left[\frac{\pi}{\tau}(t - t_i)\right], \quad (25)$$

$$\frac{dh}{dt} = 0. \quad (26)$$

Thus, over flat terrain where no topographically induced mass divergence occurs from the CBL, the inversion is destroyed solely by the growth of a CBL. Performing integrations on (25) as described in the previous section results in the analytical expression

$$H(t) = \left\{2\frac{\theta}{T}\frac{\tau}{\pi}\frac{A_0A_1}{\rho c_p\gamma}\left[1 - \cos\frac{\pi}{\tau}(t - t_i)\right]\right\}^{1/2}, \quad (27)$$

and an expression for the breakup time,

$$t_D - t_i = \frac{\tau}{\pi}\cos^{-1}\left(1 - \frac{T}{\theta}\frac{\rho c_p\gamma}{A_0A_1}\frac{\pi}{\tau}\frac{h_i^2}{2}\right). \quad (28)$$

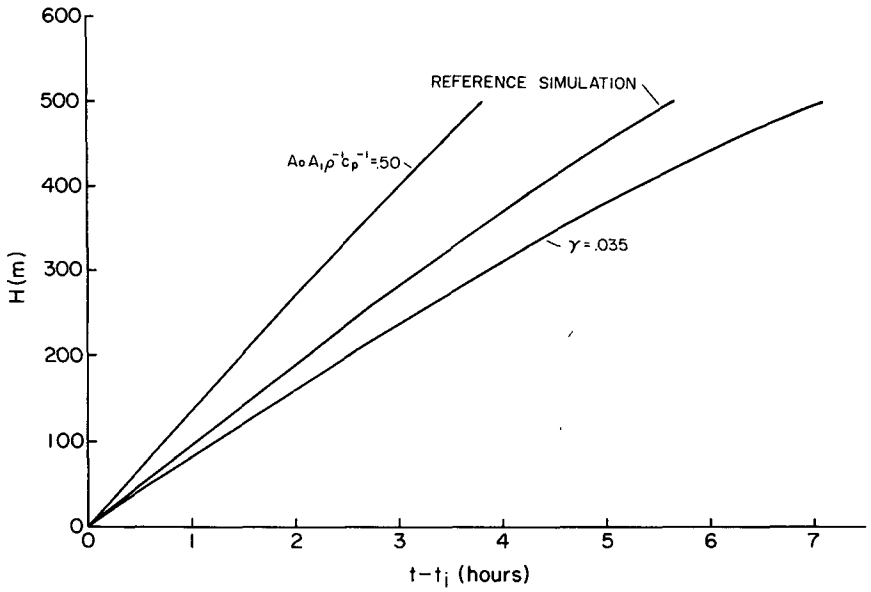

FIG. 5. Growth of CBL over flat terrain as a function of time for the modified reference inversion ($\alpha = 0$, $l \rightarrow \infty$) and for two simulations in which single parameters were changed to the values indicated. Pattern 1 destruction.

Eq. (27) is nearly identical to an equation for CBL growth over homogeneous terrain as derived by Leahey and Friend (1971). Following (27), Fig. 5 presents plots of H vs time for the reference simulation and for two cases where one parameter in the reference simulation has been changed. The reference inversion is destroyed in 5.65 h by a near-linear increase in the depth of the CBL. If the incoming energy is doubled, the inversion takes 3.8 h to break, and if the potential temperature gradient is increased to 0.035 K m^{-1}, the inversion is broken in ~7.1 h. Fig. 6 indicates the sensitivity of the time required to break an inversion on the different parameters of (28). The effect on the breakup time of changing individual parameters in the reference simulation is obtained by following the individual curves.

e. *Pattern 3 inversion destruction*

A simulation of Pattern 3 inversion destruction uses the general model [Eqs. (15) and (16)], in which a partitioning of energy is required to allow both CBL growth and inversion top descent. In order to use the general model equations, the fraction of sen-

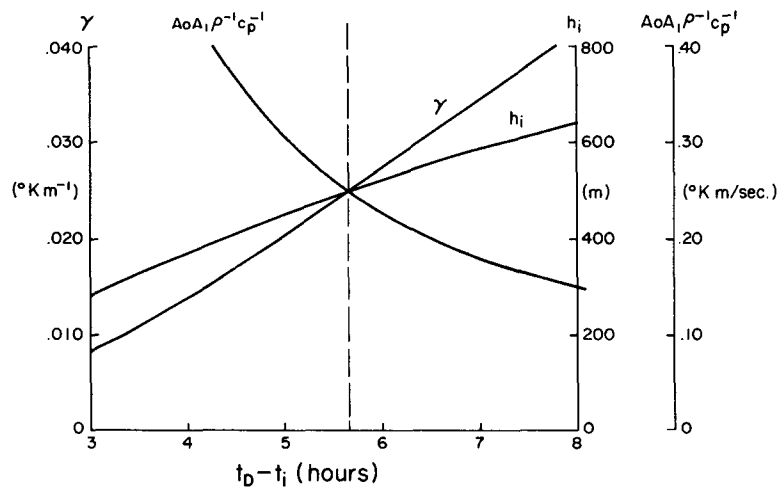

FIG. 6. Sensitivity of inversion destruction time to various model parameters for Pattern 1 inversion destruction over flat terrain.

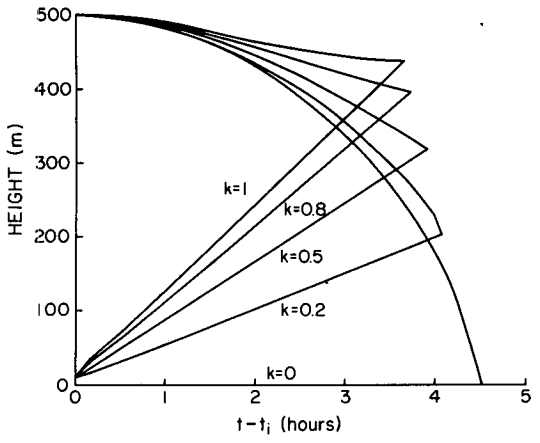

FIG. 7. Ascent of CBL and descent of inversion top as a function of time for Pattern 3 destruction of the reference inversion for different values of k.

sible heat flux $K = k[(l + HC)/(l + hc)]$ that drives the growth of the CBL must be determined. It is apparent that the fraction K is a function of time, since the initial energy input must be used primarily to develop the CBL's before appreciable mass can be carried up them. Factor K also depends on the topographic characteristics of the valley, since K must approach 1 as the valley width approaches infinity. It seems probable that K may also be a function of sensible heat flux. Since the functional dependencies of K are not yet known, it is assumed that k is a constant and, by comparing model simulations to actual data, the constant value of k that results in the best fit to data is determined. This approach allows an investigation of the effect of k on the simulation. Further research is necessary to determine the actual functional form of K, so that a better understanding of the energy partitioning phenomenon can be obtained, resulting in more accurate simulations.

The equations used to simulate Pattern 3 destruction are thus

$$\frac{dH}{dt} = \frac{\theta}{T}\frac{k}{\rho c_p}\left(\frac{l + HC}{l + \tfrac{1}{2}HC}\right)\frac{A_0A_1}{\gamma H} \times \sin\left[\frac{\pi}{\tau}(t - t_i)\right], \quad (29)$$

$$\frac{dh}{dt} = -\frac{\theta}{T}\frac{1}{\rho c_p}\left[\frac{l + hC - k(l + HC)}{l + \tfrac{1}{2}hC}\right]\frac{A_0A_1}{\gamma h} \times \sin\left[\frac{\pi}{\tau}(t - t_i)\right], \quad (30)$$

where

$$0 \leqslant (k = \text{constant}) \leqslant 1. \quad (31)$$

These equations can be integrated numerically to determine how H and h vary with time from a given initial state. Fig. 7 shows several numerical integrations using this method, time steps of 10 min, the reference simulation, and several values of k. Replotted on the same figure are some of the limiting cases of the general equations for destruction of the reference inversion discussed earlier. The time required to break the reference inversion decreases from 4.4 to 3.7 h as the value of k is increased from 0 to 1. For all values of k the growth of the CBL is nearly linear.

Fig. 8 shows the effect of varying individual parameters in the reference simulation with k fixed. The inversion is destroyed when the ascending CBL and the descending inversion top meet at a height of $H_D = h_D = 205$ m. The fact that the fraction k uniquely determines the height at which the ascending CBL meets the descending inversion top at the time of inversion destruction, suggests a means of fitting the model results to actual data that will be used in a later section.

f. Model modification to account for warming of the neutral layer

Field observations show that the potential temperature θ_h at the top of the inversion usually increases slowly with time. The warming rate varies from valley to valley and from day to day with the average warming rate being about 0.4 K h^{-1}. From the physical hypothesis, this warming requires that more energy be spent to move mass up the sidewalls, since the parcels must be warmed to a higher temperature $\theta_h(t) = \theta_h(t_i) + (d\theta_h/dt)\delta t$ to be removed from the valley. The energy requirement can be cal-

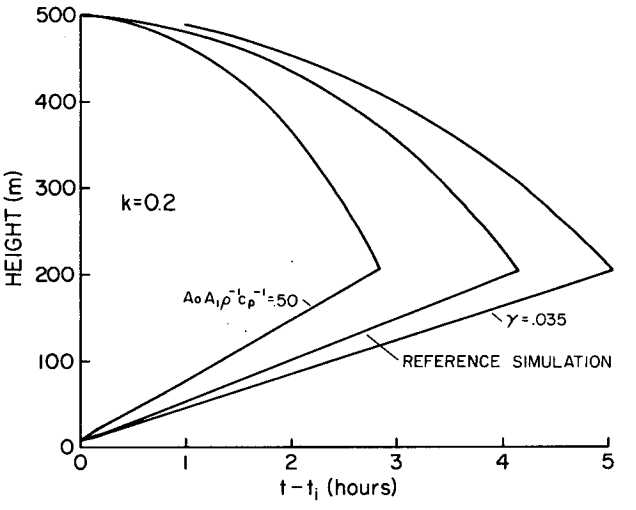

FIG. 8. Ascent of CBL and descent of inversion top for Pattern 3 destruction ($k = 0.2$) of the reference inversion, and for two simulations in which single parameters were changed to the values indicated.

culated by considering that the mass of air removed from the valley to allow the top of the inversion to sink from h_i to h is given by

$$\text{mass removed} = \rho V = \rho(h_i - h)[l + \tfrac{1}{2}(h_i + h)C], \quad (32)$$

and that the energy required to move this mass across a potential temperature jump at the top of the inversion, $\theta_h(t) - \theta_h(t_i)$ can be approximated by

$$Q_4 = \rho V c_p \frac{T}{\theta} \tfrac{1}{2}[\theta_h(t) - \theta_h(t_i)]. \quad (33)$$

If the warming in the neutral layer occurs linearly in time, the potential temperature jump is given by $\beta(t - t_i)$ where $\beta = \partial\theta_h/\partial t$ is the rate of warming. Then

$$Q_4 = \rho c_p \frac{T}{\theta}\frac{\beta}{2}(h_i - h)(t - t_i) \times [l + \tfrac{1}{2}(h_i + h)C], \quad (34)$$

$$\frac{dQ_4}{dt} = \rho c_p \frac{T}{\theta}\frac{\beta}{2}\left[(h_i - h)[l + \tfrac{1}{2}(h_i + h)C] - (t - t_i)\frac{dh}{dt}(l + hC)\right]. \quad (35)$$

The model equations are modified to account for this extra energy requirement by specifying that the fraction $k[(l + HC)/(l + hC)]$ of the inversion energy input dQ_1/dt drives the CBL growth, or

$$k\left(\frac{l + HC}{l + hC}\right)\frac{dQ_1}{dt} = \frac{dQ_2}{dt}, \quad (36)$$

while the remainder of the energy input drives the descent of the inversion and carries parcels across the potential temperature jump, such that

$$\left[1 - k\left(\frac{l + HC}{l + hC}\right)\right]\frac{dQ_1}{dt} = \frac{dQ_3}{dt} + \frac{dQ_4}{dt}. \quad (37)$$

Substituting Eqs. (12), (13), (14) and (35), the modified model equations are

$$\frac{dH}{dt} = \frac{\theta}{T}\frac{k}{\rho c_p}\left(\frac{l + HC}{l + \tfrac{1}{2}HC}\right)\frac{A_0 A_1}{\gamma H}\sin\left[\frac{\pi}{\tau}(t - t_i)\right], \quad (38)$$

$$\frac{dh}{dt} = -\frac{\theta}{T}\frac{1}{\rho c_p} \times \left\{\frac{[l + hC - k(l + HC)]A_0 A_1 \sin\frac{\pi}{\tau}(t - t_i) - \rho c_p \frac{T}{\theta}\frac{\beta}{2}(h_i - h)[l + \tfrac{1}{2}(h_i + h)C]}{h\gamma(l + \tfrac{1}{2}hC) + \tfrac{1}{2}\beta(t - t_i)(l + hC)}\right\}. \quad (39)$$

These equations can be used to simulate inversion breakup when significant warming occurs in the neutral layer above. Eq. (39) reduces to (30) when β is zero. It is important to note that (38) has the same *form* as before but, since more energy is required to move mass up the sidewalls, the partitioning of energy may be affected. If this actually occurs in nature, then the functional dependency of K is more complicated than previously discussed, since it will depend not only on time, energy input and valley width, but also on the rate of warming of the neutral layer above the inversion. As before, Eqs. (38) and (39) may be integrated numerically to simulate valley inversion breakup if $\theta_h(t)$ is known. If θ_h does not vary with time, Eqs. (29) and (30) can be used for the simulation.

3. Comparison of model results with data

In this section a finite difference form of the model equations (38) and (39) will be applied to simulate actual data collected in the valleys of western Colorado. The input parameters needed to solve the equations are given in Table 1 along with a summary of how they may be obtained. The output of the model is $h(t)$ and $H(t)$. From these outputs and the assumptions that γ is constant for altitudes between H and h, that potential temperature is independent of height in the CBL and neutral layer, and that $\theta_h(t_i)$ and $\partial\theta_h/\partial t$ are known, $\theta(t, z)$ for the CBL, stable core and neutral layer can be determined. Unfortunately, since two of the input parameters to the thermodynamic model (k and A_0) were not observed in the field programs, the equations cannot be applied directly. Instead, arbitrary values for k and A_0 are chosen until the best simulation of the data is obtained with the model. It is then determined whether the values of k and A_0 are reasonable for the situation at hand. Both k and A_0 are bounded, since they are fractions between 0 and 1. The value of k specifies the constant fraction of sensible heat flux that is used to cause the CBL to deepen. The model results are presented below for a winter Pattern 2 inversion destruction in the wide Yampa Valley and for a fall Pattern 3 inversion destruction in the Eagle Valley.

a. Pattern 2 simulation—Yampa Valley, 23 February 1978

The model input parameters required to simulate the Pattern 2 inversion destruction observed in the snow covered Yampa Valley on 23 February 1978 were obtained as follows. First, $\theta T^{-1} = 1.07$ and $\rho c_p = 1040$ J m^{-3} K^{-1} were calculated using the ap-

TABLE 1. Model input parameters.

Model input			Source
Constants	(i)	θ/T	from average P and T of valley atmosphere
	(ii)	ρC_p	
Valley topography	(iii)	l	from topographic maps
	(iv)	C	
Initial inversion characteristics	(v)	γ	from sunrise sounding
	(vi)	h_i	
Solar irradiance	(vii)	A_1	from extraterrestrial solar irradiance model or field notes for t_i
	(viii)	τ	
	(ix)	t_i	
External conditions (neutral layer warming)	(x)	β	from sequential soundings taken during observation of inversion breakup or from climatic data
Energy partition	(xi)	k	comparisons of theory and data
Surface energy balance	(xii)	A_0	measurements, if available
Numerical	(xiii)	$H_i \neq 0$	arbitrary
	(xiv)	Δt	

proximate mean pressure (780 mb) of the early morning inversion and an average temperature of the valley atmosphere (−10°C) from the defining equation for potential temperature and from the equation of state, respectively. Second, the valley topographic parameters (l = 2580 m, α_1 = 9°, α_2 = 16°, C = 9.80) were obtained from topographic maps. Third, the initial inversion parameters (h_i = 530 m, γ = 0.0345 K m^{-1}) were estimated from a straight line fit to the top of the 0714 MST sounding on this date. The hyperbolic lower region of the sounding could not be adequately fit with a straight line, so it is ignored in the analysis. Fourth, a sinusoidal fit to the extraterrestrial solar flux curve obtained from a standard solar irradiance model (e.g., Sellers, 1965) provides solar irradiance parameters (A_1 = 878 W m^{-2}, t_i = 0655 MST, τ = 10.9 h). The output of the solar irradiance model for the horizontal surface of interest is presented in Fig. 9. For reference, the solar fluxes on extraterrestrial surfaces with the same aspect and inclination angles as the valley sidewalls are indicated on the figure. The input required to run the solar irradiance model includes the date and the latitude and longitude of the Yampa Valley site. The remaining parameters necessary to run the inversion destruction model are fractions k and A_0, and the neutral layer warming rate β. To simulate a Pattern 2 destruction, k must be zero. The neutral layer warmed only 1.1 K during the inversion destruction, for a warming rate β of 2.8 × 10^{-5} K

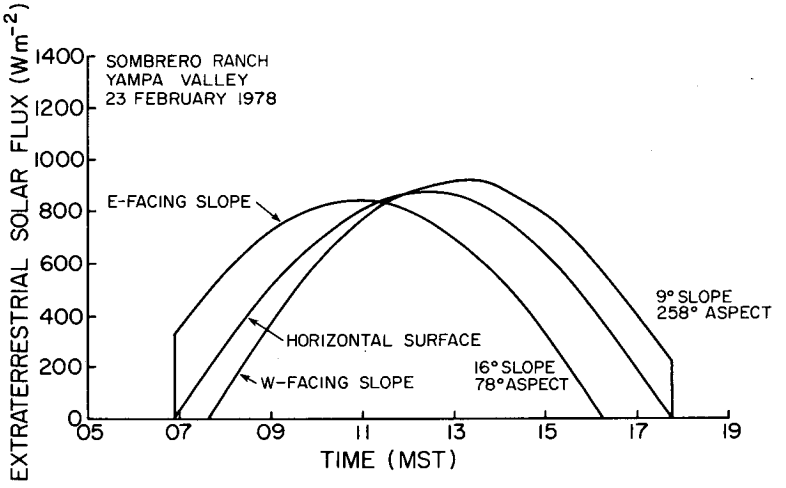

FIG. 9. Extraterrestrial solar flux calculated for valley floor and sidewall surfaces of the Yampa Valley, 23 February 1978.

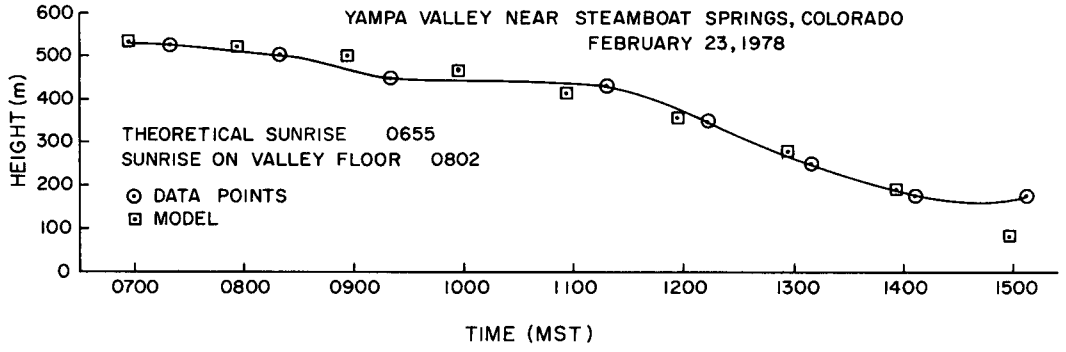

FIG. 10. Comparison of model simulation of $h(t)$ with actual data for the Yampa Valley, 23 February 1978.

s^{-1}. The best fit of the model output $h(t)$ to the inversion top data of Fig. 10 was obtained with $A_0 = 0.19$ by a trial-and-error procedure. Using this value, the simulation of the height of the top of the inversion agrees to within 25 m of the data over a 7 h period. In mid-afternoon, however, the simulation continues to call for the descent of the inversion top, when the actual data indicate that the descent stopped. This is probably due to afternoon shading of the valley by a mountain peak southwest of the site. The model, using a simple sine function to simulate solar flux, does not account for this shading. In Fig. 11 the potential temperature profile simulations are compared to actual sounding data. The sounding data consist of eight consecutive potential temperature soundings taken at ~1 h intervals throughout the day. The characteristics of the initial inversion were obtained from the 0714 MST sounding and are indicated by the straight line fit to the sounding in the figure. The slow neutral layer warming is also apparent in the figure. The excellent fit of the model simulations to the data in the stable core above the 50 m deep surface layer is shown for soundings 4 and 6. The value of A_0 required to obtain these results seems reasonable for the snow-covered valley with evergreen forests covering much of the valley sidewall above the observation site. It is particularly interesting that the model assumption of constant potential temperature gradient was satisfied well during the long period of inversion destruction in the complicated topography of the Yampa Valley. The case study is an excellent example of the effect of enhanced albedo due to snow cover in retarding the normal breakup of an inversion. Despite the fact that the temperature inversion was not destroyed on this clear day, the diurnal range of temperature at the ground was quite large.

b. Pattern 3 simulation—Eagle Valley, 16 October 1977

Pattern 3 inversion breakup in the Eagle Valley is remarkably consistent in all seasons when snow cover is not present in the valley. To test the mathematical model, the Pattern 3 breakup on the clear day of 16 October 1977 is chosen for simulation. The input parameters to the model are obtained as for the Pattern 2 simulation above. Thus, values of the constants θT^{-1} (1.08) and ρc_p (990 J m^{-3} K^{-1}) are determined from the approximate mean pressure (768 mb) and temperature (0°C) of the valley inversion. The valley topographic parameters ($l = 1450$ m, $\alpha_1 = 21°$, $\alpha_2 = 10°$, $C = 8.28$) are determined from topographic maps. The initial values of the inversion parameters ($h_i = 650$ m and $\gamma = 0.0269$ K m^{-1}) were taken from the 0650–0719 MST sounding since the pre-sunrise sounding was of insufficient height to determine h_i. A solar irradiance model was used to determine the parameters $A_1 = 906$ W m^{-2}, $t_i = 0621$ MST and $\tau = 11$ h (Fig. 12). The value of β (8.3×10^{-5} K s^{-1}) was taken from valley temperature sounding data.

The fitting of the model output to the data on Fig. 13 was accomplished first by choosing the value of

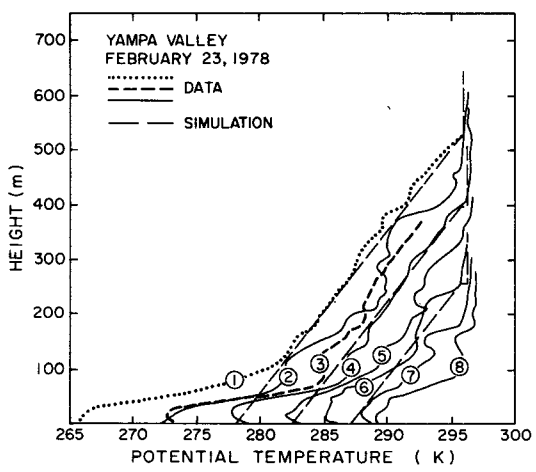

FIG. 11. Comparison of model simulation of potential temperature structure with data for the Yampa Valley, 23 February 1978. Upsoundings 1–8 were initiated at 0714, 0905, 0959, 1100, 1202, 1259, 1359 and 1508 MST, respectively.

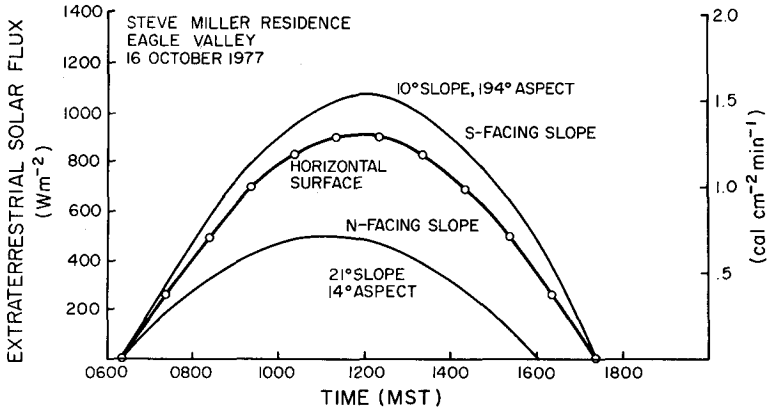

FIG. 12. Extraterrestrial solar flux calculated for valley floor and sidewall surfaces of Eagle Valley, 16 October 1977.

k so that the ascending CBL and descending inversion top met at the proper observed height at the time of inversion destruction. The value of A_0 was then varied until the model outputs $h(t)$ and $H(t)$ fit the data well. The fit in Fig. 13 was obtained with $k = 0.14$ and $A_0 = 0.45$. The value of A_0 seems realistic considering the dry nature of the valley surface on this date. The equations were integrated from the initial conditions of $h = 650$ m and $H = 10$ m at $t = 0705$ MST using a time step of 10 min. From Fig. 13 it is clear that a good fit to the data is obtained with the chosen values of the two parameters A_0 and k. The simulation of CBL height and inversion top height agrees with the data within 50 m over most of the period of inversion destruction. The CBL height was overpredicted early in the inversion period, due to the bulk nature of the model. Following sunrise, the CBL develops first over the illuminated sidewall or sidewalls, and somewhat later over the valley floor when it is sunlit. The bulk model, however, does not differentiate between CBL growth over the three different valley surfaces. All energy going into CBL growth is attributed, in the model, to growth of the valley floor CBL. Thus, the initial overprediction of CBL growth over the valley floor is a characteristic feature of the model equations. The behavior of the simulation at mid-levels of the valley atmosphere near the time of inversion destruction should also be mentioned. The data typically show a more sudden inversion breakup is to be expected in nature since the final remnants of the stable core will break up in convective overturning, once the stable core becomes thin enough and the convective plumes rising from the valley floor become vigorous enough. Due to the chaotic nature of the breakup, actual soundings taken during this time will often show deformations in the vertical potential temperature profiles. Estimates of heights h and H from soundings are difficult to make during this time. A continued flux of energy into this region is nec-

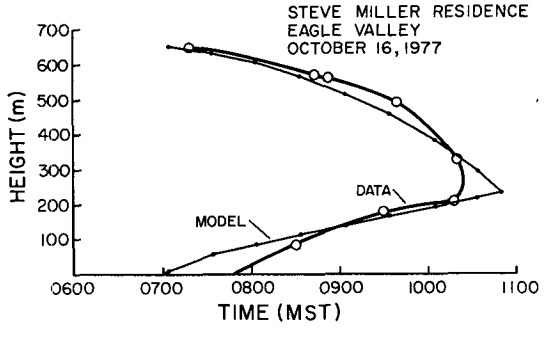

FIG. 13. Comparison of model simulation of $H(t)$ and $h(t)$ with actual data for the Eagle Valley, 16 October 1977.

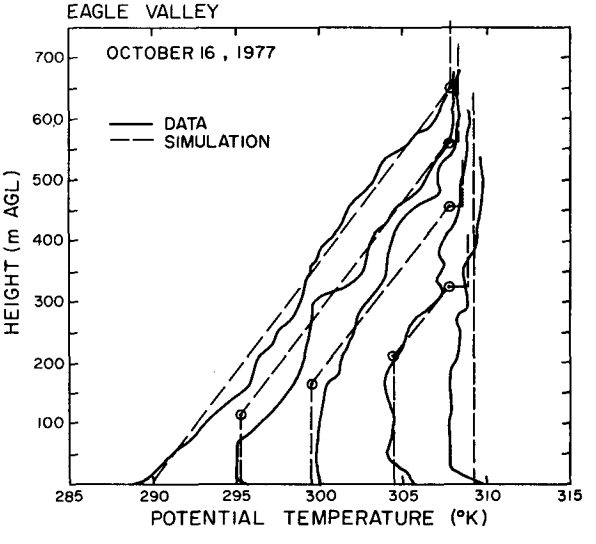

FIG. 14. Comparison of model simulation of potential temperature structure with data from the Eagle Valley, 16 October 1977.

essary before the deformations in the profiles are destroyed and well-organized convection through the entire depth of the valley results in smooth neutral profiles. When this occurs, the breakup can be considered as finished.

The potential temperature profiles corresponding to the data and simulation of Fig. 13 are presented in Fig. 14. The potential temperature data are from the tethersonde up-soundings taken at 0650–0719, 0829–0848, 0924–0948, 1013–1033 and 1106–1121 MST. The corresponding potential temperature simulations are plotted for the approximate midtimes of the tethersonde up-soundings at 0840, 0935, 1025 and 1115. Again, the model provides a good simulation of the actual data, reproducing the warming and growth of the CBL, the warming of the stable core, and the descent of the inversion top.

4. Summary and conclusions

A thermodynamic model of valley temperature structure evolution has been developed. By differentiating the first law of thermodynamics, the rate of energy input into the valley atmosphere is equated to the rate of descent of the inversion top and the rate of ascent of the CBL under the following assumptions:

1) The potential temperature gradient in the stable core is constant during the period of inversion breakup.

2) The temperature structure is horizontally homogeneous in the cross-valley direction.

3) The valley topography can be adequately represented by a horizontal valley floor of arbitrary width and two linear sidewalls of arbitrary slope.

4) The initial inversion at sunrise can be adequately represented by a constant potential temperature gradient layer of arbitrary depth.

5) Convective boundary layers can be adequately represented as constant potential temperature layers of arbitrary height.

6) The rate of energy input into the valley atmosphere is a constant fraction of the solar energy flux (assumed to be a sinusoidal function of time from sunrise to sunset) coming across the horizontal upper surface of the inversion.

To complete the model, the partitioning of the energy input into CBL growth and mass transport must be estimated. As a first approximation, it is assumed that a constant fraction of the energy input is used to cause the CBLs to grow. The remaining energy is used for mass transport in the upslope flows. Energy going into the growth of the CBL causes the CBL depth to increase with time. Energy causing air parcels to flow up the sidewall CBLs results in the descent of the top of the inversion. When most of the available energy drives the growth of the CBLs, a temperature structure evolves in which the inversion is destroyed predominantly by the upward growth of a CBL from the ground. When most of the available energy drives mass up the sidewalls, a temperature structure evolves in which the inversion is destroyed by the descent of the inversion top.

The inputs to the model are 1) the initial inversion characteristics (depth and average potential temperature gradient); 2) valley topography (floor width and inclination angles of the two sidewalls); 3) the rate of energy input; and 4) the fraction of energy available to increase the depth of the CBL. The effect on inversion evolution of warm air advection above the inversion layer can be investigated by using a modified version of the model in which the warming rate is input.

The model simulates the changes with time of the height of the inversion top and the depth of the CBL during the inversion breakup period. From these simulations potential temperature profiles of the valley atmosphere can be constructed for any time during the period.

Sensitivity analyses were conducted for the limiting cases of the model. The results indicate that the time required to destroy an inversion depends primarily on the initial height of the inversion, on its potential temperature gradient, and on the amount of energy available to destroy it. Using a reference simulation in which model parameters were given values typical of valley inversions, inversion destruction took approximately 3½ to 4½ h after sunrise. These times correspond well with actual observations. Less time is required to destroy a valley inversion than an inversion of like dimensions over the plains, because the available energy is used to warm a smaller volume of air. For the dry valleys of western Colorado, the amount of energy available depends to a large extent on the presence or absence of snow cover or surface moisture in the valley. Valley inversions were destroyed sooner by the growth of a CBL than by the descent of the inversion top. Valley width and inclination angles of the sidewalls had only a limited effect on the time required to destroy an inversion. Increased valley width and steeper sidewalls both increased slightly the time required.

The thermodynamic model was used to simulate two specific sets of inversion breakup data for Pattern 2 and 3 temperature structure evolution in the topographically diverse Eagle and Yampa Valleys. Simulations were obtained by fitting two constants in the model (relating to the surface energy budget and energy partitioning) to the data. The model output fit the Pattern 2 inversion breakup in the snow-covered Yampa Valley very well using an energy input equal to 19% of the extraterrestrial solar flux on a horizontal surface, and assuming that all of this energy was used to drive the slope flows. A good fit to the Eagle Valley data was obtained using an energy input equal to 45% of the extraterrestrial solar

flux and assuming that 14% of this energy was used to cause the valley floor CBL to grow. The remaining energy was used to remove mass from the valley in the slope flows.

Results of the present study provide new insights into the evolution of valley temperature structure and quantify the influence of the various parameters affecting temperature inversion breakup. The model explains the importance of the initial sunrise inversion characteristics; the observed timing of the beginning of inversion destruction; the mean time required to destroy typical inversions in the deep valleys of western Colorado; the weak seasonal dependence of the time period required to destroy the inversions; the effects of snow cover and ground moisture and of valley topography; the patterns of warming observed in the various layers of the temperature structure; the typical observed inversion top descent rates of 40–150 m h^{-1}; and the retarded growth of the valley CBL's relative to the flat plains case. The thermodynamic model, while implicitly incorporating up-slope mass transport, is able to simulate temperature structure evolution in a wide range of valley topography without taking account of along-valley wind systems.

Acknowledgments. The research was accomplished at the Department of Atmospheric Science, Colorado State University, under funding from Grant ATM76-84405, Atmospheric Sciences Section, National Science Foundation. The manuscript was prepared under funding from the Environmental Protection Agency through Interagency Agreement AD-89-F-0-097-0, with the U.S. Department of Energy.

REFERENCES

Leahey, D. M., and J. P. Friend, 1971: A model for predicting the depth of the mixing layer over an urban heat island with applications to New York City. *J. Appl. Meteor.*, **10,** 1162–1173.

Sellers, W. D., 1965: *Physical Climatology.* University of Chicago Press, 272 pp.

Whiteman, C. D., 1982: Breakup of temperature inversions in deep mountain valleys: Part I. Observations. *J. Appl. Meteor.*, **21,** 270–289.